

Short Communication

Experimental and Theoretical Prediction of The Redox Potential of Dopamine and Its Supramolecular Complex With Glycine

Meng-Meng Liu¹, Shu-Min Han¹, Xiao-Wen Zheng², Ling-Li Han^{2,3}, Tao Liu^{2,*}, Zhang-Yu Yu^{1,2,*}

¹ School of Chemistry and Chemical Engineering, Qufu Normal University, Qufu 273165, Shandong, China

² Department of Chemistry and Chemical Engineering, Key Lab of Inorganic Chemistry, Shandong Provincial Education Department, Jining University, Qufu 273155, Shandong, China

³ Key Laboratory of Theoretical and Computational Photochemistry, Ministry of Education, College of Chemistry, Beijing Normal University, Beijing 100875, China

*E-mail: liutao_2005@126.com; zhangyu_yu@126.com

Received: 18 September 2014 / Accepted: 2 November 2014 / Published: 17 November 2014

The redox reaction of catecholamine is a two-proton-two-electron reaction in aqueous solution. N-protonated dopamine (DA) can be oxidated to N-protonated dopamine quinone (DAquinone). The standard electrode potential (E°) value of DA/DAquinone couple is obtained experimentally with cyclic voltammetry (CV) and theoretically with two methods at B3LYP/6-311++G(d,p) level. The theoretical E° value of DA/DAquinone couple is in good agreement with experimental one and close to each other. Glycine (Gly) is the simplest amino acid, and it can form hydrogen bonds with DA in physiological environment. The E° value of DA-Gly/DAquinone-Gly couple is predicted experimentally and theoretically. We find that the E° value of DA-Gly/DAquinone-Gly couple is larger than DA/DAquinone couple. Hydrogen bond interaction weakens the electron-donation abilities of DA.

Keywords: dopamine; noradrenaline; standard electrode potential; cyclic voltammetry; B3LYP

1. INTRODUCTION

As one of the most important neurotransmitters in mammals, catecholamine plays an important role in the bodies [1,2]. Catecholamine includes dopamine (DA), adrenaline, and noradrenaline. The abnormal level of DA will cause a lot of diseases such as Parkinson's disease and depression [3,4]. Since electron transfer reaction is the essence of catecholamine's reaction in bodies, their biological actions are related with redox potentials tightly [5]. The studies on the electrochemical behaviors of DA are of great significance to understand its physiological functions and diagnose certain diseases in

clinical medicine. N-protonated DA (Fig. 1A) is stable under acidic conditions, which can be oxidated to N-protonated DAquinone (Fig. 1B).

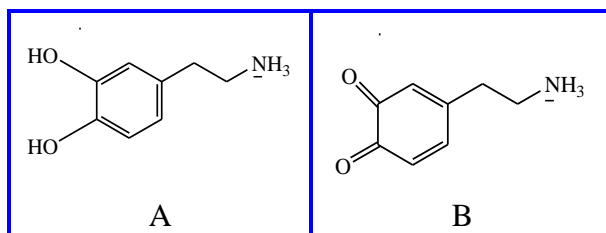


Figure 1. The structures of N-protonated DA (A) and DAquinone (B).

In the recent years, the theoretical and experimental studies of catecholamine have been increasingly deepening [6-10]. Because of its relatively high sensitivity and less time consuming, cyclic voltammetry (CV) is widely applied in the researches of catecholamine's electron-transfer reactions [11-15]. Whereas, the researches are mostly limited to the analytical detection and few can proclaim the nature of the redox reactions. In this article, CV experiments combined with theoretical calculations have been adopted to predicate E° of DA/DAquinone couple. Firstly, the conditional formal electrode potential (E°) values of DA/DAquinone couple at different temperature and pH values have been measured with CV. Thermodynamic functions and E° are calculated theoretically, and compared with the experimental results. Then, we select glycine (Gly) as the model molecule to calculate the E° values of DA-Gly/DAquinone-Gly couple and study the electron transfer properties of DA in physiological environment.

2. EXPERIMENTAL SECTION

2.1. Instrumentation and reagents

Electrochemical measurements were carried out using a CHI 660C electrochemical station. A three-electrode electrochemical cell was employed for all the electrochemical measurements. A glassy carbon electrode (GCE) with a diameter of 1.5 mm as a working electrode, while the counter and reference electrodes were platinum wire electrode and saturated calomel reference electrode (SCE), respectively. All experimental potentials we obtained directly from cyclic voltammograms were relative to SCE. The phosphate buffer solutions were prepared from 0.1 mol L⁻¹ citric acid and 0.2 mol L⁻¹ Na₂HPO₄ according to the buffer preparation table and justified by a Metrohm 691 pH/mV meter. All solutions were prepared with analytic grade reagents and doubly distilled water. 0.1 mol L⁻¹ KCl solution worked as supporting electrolyte during the whole experiment.

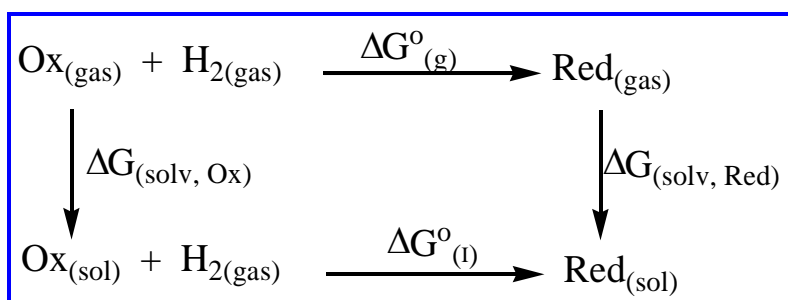
2.2. Electrode preparation

In order to obtain a clean renewed electrode surface, GCE was polished with fine wet emery papers and then cleaned by successive polishing with 0.3 and 0.05 μm Alumina–water slurry prior to its use in electrochemical experiments. A Luggin capillary was used to connect the reference and working electrodes in order to reduce the solution resistance. Highly pure nitrogen was passed through the solution for 15 min to remove dissolved oxygen in solution before measurements, and all experiments were carried out under nitrogen atmosphere in a double-walled electrolytic tank connected to a thermostatic water bath.

3. THEORETICAL SECTION

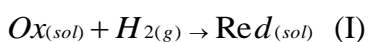
All calculations have been carried out with Gaussian 09 package [16] at B3LYP/6-311++G(d,p) theoretical level. The most stable molecular geometries optimized fully have been selected according to the free energy in gas phase and in aqueous solution, respectively. Harmonic vibrational frequencies were also calculated at the same level of theory to identify all stationary points as minima (zero imaginary frequencies). The continuum model of solvation, the conductor-like polarizable continuum model (CPCM) [17-19], was used to derive the solvation free energies with the UAKS radii at the B3LYP/6-311++G(d,p) level of theory. Two methods were employed to calculate the standard potentials E° of DA and DA-Gly.

3.1. Method I



Scheme 1. Thermochemical cycle for method I.

The oxidation of catecholamine is a two-electron-oxidation reaction in aqueous solution. The transformation from oxidation state (Ox) to reduction state (Red) can be described with the following reaction



To obtain E° , the total change of Gibbs free energy ΔG° for the reaction I is demanding to be calculated. Therefore, a thermodynamic cycle (see Scheme 1) is established to calculate the total change of Gibbs free energy $\Delta G^\circ_{(\text{l})}$.

From this thermochemical cycle, it is not hard to compute $\Delta G^o_{(l)}$ from its components by the following formula:

$$\Delta G^o_{(l)} = \Delta G^o_{(g)} + \Delta G_{(solv)} \quad (1)$$

In equation 1, $\Delta G^o_{(g)}$ and $\Delta G_{(solv)}$ is the change of standard Gibbs energy in the gas phase and the change of solvation energy in aqueous solution, respectively. $\Delta G^o_{(g)}$ and $\Delta G_{(solv)}$ are defined as follows:

$$\Delta G^o_{(g)} = G^o_{(g,Red)} - G^o_{(g,Ox)} - G^o_{(g,H_2)} \quad (2)$$

$$\Delta G_{(solv)} = \Delta G_{(solv,Red)} - \Delta G_{(solv,Ox)} \quad (3)$$

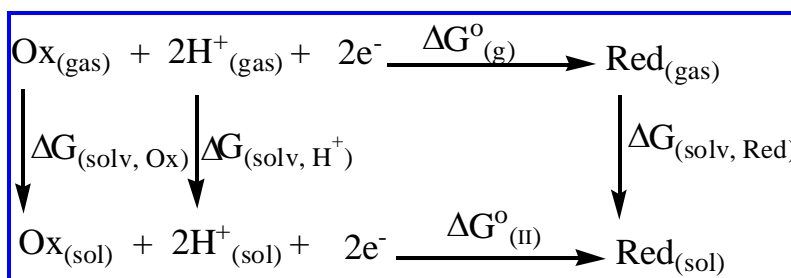
$G^o_{(g,Red)}$ and $G^o_{(g,Ox)}$ are the Gibbs free energies of Red and Ox calculated accurately using the 6-311++G(d,p) basis set at the B3LYP level of theory in gas phase. $G^o_{(g,H_2)}$ is calculated as $-1.180997 \text{ kcal mol}^{-1}$ at the B3LYP/6-311++G(d,p) level. $\Delta G_{(solv,Red)}$ and $\Delta G_{(solv,Ox)}$ are the solvation free energies of Red and Ox in aqueous solution obtained using the CPCM model with UAKS radii at the B3LYP/6-311++G(d,p) level of theory.

The thermodynamic parameters link to standard redox potential E^o relative to the standard hydrogen electrode (SHE) via the Eq. 4.

$$\Delta G^o_{(l)} = -nFE^o \quad (4)$$

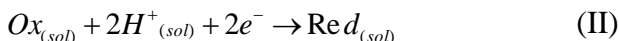
Where n is the number of the transferred electrons in reaction, and F is Faraday constant (96485 C mol^{-1} or $23.061 \text{ kcal mol}^{-1} \text{ V}^{-1}$) [15], respectively. The E^o value of SHE is equal 0.00 V in SI units.

3.2. Method II



Scheme 2. Thermodynamic cycle for method II.

Besides the expression of reaction I, the transformation of Ox converting to Red can be put as the following two-electron half-cell reaction, too.



Similar to method I, the total change of Gibbs free energy ΔG^o for the reaction II ought to be calculated first from the introduced cycle scheme 2.

$$\Delta G^o_{(II)} = \Delta G^o_{(g)} + \Delta G_{(solv,Red)} - \Delta G_{(solv,Ox)} - \Delta G_{(solv,H^+)} - n\Delta G^{o \rightarrow *}$$

In Eq. 5, $\Delta G^{\circ}_{(m)}$ stands for the total change of free energy for reaction II. $\Delta G^{o \rightarrow *}$ is an adjusted value for the reactions shifting from one atmosphere in gas phase to 1 mol L^{-1} in solution and it is regarded as $1.9 \text{ kcal mol}^{-1}$ (or 7.9 kJ mol^{-1}) for each component [20].

Note that $\Delta G^{\circ}_{(m)}$ is different from $\Delta G^{\circ}_{(1)}$. If $\Delta G^{\circ}_{(m)}$ is divided by $-nF$, the result value is the absolute redox potential instead of the standard redox potential E° . The absolute reductive potential of SHE 4.44 V [15] should be taken into consideration when we calculate theoretical E° via Eq. 4.

The calculated systematic errors on reactants and products will be counteracted mostly while calculating ΔG° and we need not take the effect of pH into consideration and water is regarded as the solvent in the CPCM model of solvation in the present work.

3.3. Thermodynamic analysis

The following Eq. 6 works as a role of a bridge to associate theoretical potential E° with experimental studies.

$$E^{\circ'} = E^{\circ} - 2.303(mRT/nF) \text{ pH} \quad (6)$$

where T is temperature, R is gas constant and F is Faraday constant ($23.061 \text{ Kcal mol}^{-1} \text{ V}^{-1}$) [15], respectively. n and m are the number of electrons and protons transferred in this reaction. Both n and m equal to 2 here. If the conditional formal electrode potential $E^{\circ'}$ here is relative to SHE, then E° is relative to SHE. Similarly, if $E^{\circ'}$ here is relative to SCE, then E° is relative to SCE. In experimental studies, as predecessors did [21,22], we regard $E^{\circ'}$ as half of the sum of the anodic peak potential E_{pa} and the cathodic peak potential E_{pc} .

$$E^{\circ'} = (E_{pa} + E_{pc})/2 \quad (7)$$

In equation 7, the $E^{\circ'}$ is relative to SCE for the anodic peak potential E_{pa} and cathodic peak potential E_{pc} are measured with CV directly.

As for the experimental thermodynamic functions, the slope of the liner E° (vs SHE) vs temperature is demanding to be found according to Eqs. 8 and 9. Subsequently, experimental values of ΔS° , ΔH° and ΔG° are obtained.

$$\Delta S^{\circ} = nF(\partial E^{\circ}/\partial T)_P \quad (8)$$

$$\Delta H^{\circ} = -nF[E^{\circ} - T(\partial E^{\circ}/\partial T)_P] \quad (9)$$

$$\Delta G^{\circ} = \Delta H^{\circ} - T\Delta S^{\circ} \quad (10)$$

4. RESULTS AND DISCUSSION

4.1. Influence of temperature on DA voltammetric response

To derive the thermodynamic parameters, the effect of temperature on the standard redox potential E° (vs SHE) has been investigated in the solution containing $5.2 \times 10^{-3} \text{ mol L}^{-1}$ DA at fixed pH 3.2 with a scan rate of 100 mV/s (Fig. S1). Note that the values of E° are obtained via the Eq. 6, and $E^{\circ'}$ (vs SHE) is the mean value at each temperature. The exact potential value of SCE vs SHE varies with temperature at constant pressure [23]. $E^{\circ'}$ (vs SHE) of DA/DAquinone couple decreases with the

increase of temperature. $(\partial E^\circ/\partial T)_P$ is the slope of line E° vs temperature shown in Fig. 2. E° and $E^{\circ'}$ of DA/DAquinone couple, and thermodynamic functions are listed in Table 1 in detailed. The delta entropy ΔS° of $-60.88 \text{ cal mol}^{-1} \text{ k}^{-1}$ is independent of the temperature. The delta enthalpy ΔH° is temperature-irrelative according to the previous reports [19,24], so we consider the mean change of ΔH° $-55.08 \text{ kcal mol}^{-1}$ as the accurate ΔH° . The total free energies ΔG° increases with the temperature increasing.

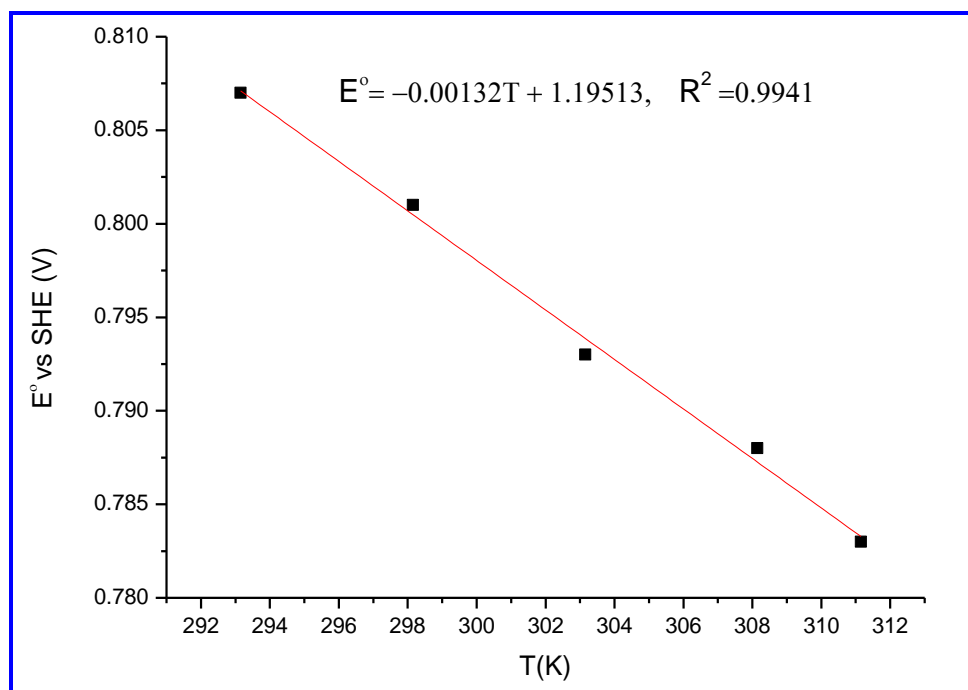


Figure 2. The plot of E° (vs SHE) of DA/DAquinone couple vs temperature.

Table 1. Experimental redox potentials and thermodynamic functions for electrochemical reaction of DA in a phosphate buffer solution (pH=3.2) in the range of 20 to 38°C (293.15-311.15 K)

Property	293.15 K	298.15 K	303.15 K	308.15 K	311.15 K
$E^\circ_{\text{SCE}}/\text{V}^a$	0.248	0.244	0.241	0.238	0.236
$E^{\circ'}(\text{vs SCE})/\text{V}^b$	0.370	0.368	0.363	0.361	0.358
$E^{\circ'}(\text{vs SHE})/\text{V}^b$	0.618	0.612	0.604	0.599	0.594
E°/V^c	0.807	0.801	0.793	0.788	0.783
$\Delta H^\circ/\text{Kcal mol}^{-1}$	-55.07	-55.10	-55.07	-55.10	-55.06
$\Delta S^\circ/\text{cal mol}^{-1} \text{ k}^{-1}$	-60.88				
$\Delta G^\circ/\text{Kcal mol}^{-1}$	-37.22	-36.94	-36.57	-36.34	-36.11

^aThe exact potential values of SCE at each temperature.²³

^bThe conditional redox potentials at pH 3.2.

^cThe standard redox potentials vs SHE at pH 0.

4.2. Influence of pH on DA voltammetric response

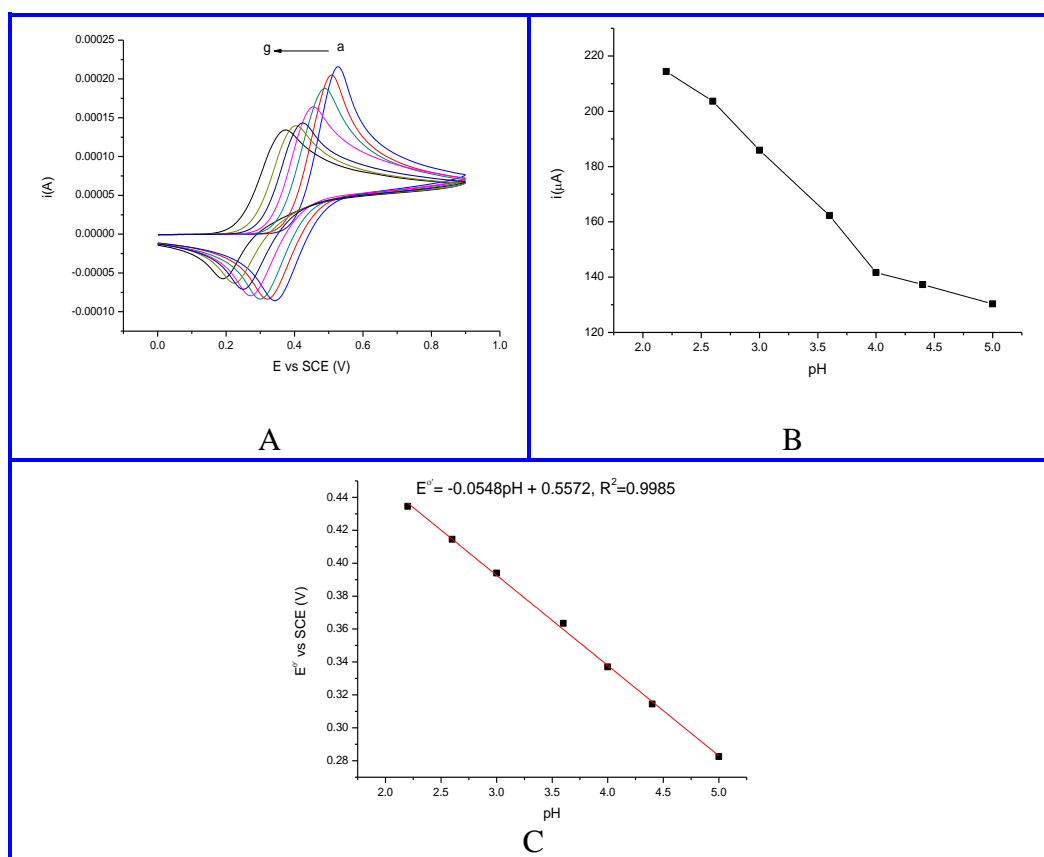


Figure 3. (A) The CV behaviors of $5.2 \times 10^{-3} \text{ mol L}^{-1}$ DA at GCE in phosphate buffer solution with different pH values at a scan rate of 100 mV/s (curves a to g: pH=2.2, 2.6, 3, 3.6, 4, 4.4, 5). (B) The plot of anodic peak current i_{pa} vs pH. (C) The plot of $E^{o'}$ (vs SCE) vs pH.

The DA response is investigated by CV in a phosphate buffer solution containing $5.2 \times 10^{-3} \text{ mol L}^{-1}$ DA at various pH values ranging from 2.2 to 5.0 at room temperature with the scan rate of 100 mV/s (Fig. 3A). The ionic strength is adjusted by KCl. Fig. 3B shows that current responses decrease with the increase of pH. The concentration of H^+ in the pH range we studied is larger, the oxidation of DA is easier. As the primary ionization constant for the phosphoric acid system is 7.52×10^{-3} [25], the quantity of H_2PO_4^- will increase gradually with the increase of solution pH in the range of 2.2 to 5.0. H_2PO_4^- in the system can form supramolecular complexes with N-protonated DA through hydrogen bond and ion-dipole interactions, which will protect DA to be oxidized and result into the anodic peak current decreases with the pH from 2.2 to 5.0.

The conditional formal potential, $E^{o'}$ (vs SCE), is derived from the voltammograms via the Eq. 7. $E^{o'}$ is pH dependent and shifts to negative potential as pH increases, which can be seen from Fig. 3C. The equation of fit line in Fig. 3C is

$$E^{o'} = -0.0548 \text{ pH} + 0.5572 \quad (11)$$

By contrasting Eq. 11 with Eq. 6, it is not hard to find that the experimental E^o (pH=0) is 0.5572 V relative to SCE at 298.15K (E^o of SCE is 0.244 V at room temperature) [23]. Thus the

experimental E° relative to SHE is 0.801 V. The slope of -0.0548 V per unit of pH is close to the theoretically anticipated Nernstian value of -0.059 V/pH, which indicates that the redox reaction of DA is a two-electron-two-proton process.

4.3. The theoretical prediction of E° of DA/DAquinone redox couple

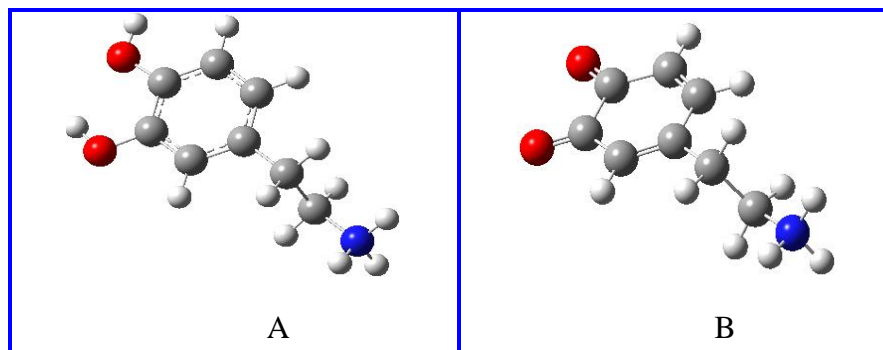


Figure 4. The most stable structures of DA (A) and DAquinone (B) optimized in aqueous solution at the B3LYP/6-311++G(d,p) level.

All structures of DA and DAquinone have been optimized fully in the gas phase and aqueous solution at B3LYP/6-311++G(d,p) level to guarantee the rationality of the theoretical calculations. The most stable structures of DA and DAquinone in aqueous solution are shown in Fig. 4.

Table 2. Calculated gas-phase energies $G^\circ(\text{g})$ and solvation energies $\Delta G(\text{solv})$ of studied species, Gibbs free energy (ΔG°) of the studied reactions, and redox potentials (E°) of DA/DAquinone and DA-Gly/DAquinone-Gly calculated with methods I and II at B3LYP/6-311++G(d,p) level.

B3LYP/6-311++G(d,p)	$G^\circ(\text{g})$ (Hartree)	$\Delta G(\text{solv})$ (kcal mol ⁻¹)	Method I		Method II		$E^\circ(\text{expt})^a$ (V)
			$\Delta G^\circ_1/\Delta G^\circ_3$ (kcal mol ⁻¹)	E°_1/E°_3 (calcd) (V)	$\Delta G^\circ_2/\Delta G^\circ_4$ (kcal mol ⁻¹)	E°_2/E°_4 (calcd) (V)	
DA	-517.03	-92.29					
DAquinone	-515.78	-99.57					
DA/DAquinone			-36.06	0.782	-242.38	0.815	0.801
DA-gly	-801.523	-103.84					
DAquinone-gly	-800.283	-102.04					
DA-gly/DAquinone-gly			-38.5733	0.836	-244.8988	0.869	0.819

^aThe experimental standard potential values vs SHE at room temperature.

The theoretical calculated gas-phase Gibbs energies $G^\circ(\text{g})$ of each component and solvation energies $\Delta G(\text{solv})$ calculated using CPCM model of solvation at B3LYP/6-311++G(d,p) theoretical level are listed in Table 2. Furthermore, the total changes of Gibbs free energy for reductive reaction I and II from Ox DAquinone to Red DA, ΔG°_1 and ΔG°_2 , are calculated via Eqs. 2 and 5, respectively.

The theoretical standard redox electrode potentials $E^\circ(\text{calcd})$ for DA/DAquinone redox couple using methods I and II, $E^\circ_1(\text{calcd})$ and $E^\circ_2(\text{calcd})$, are derived via Eq. 4 also shown in Table 2, where the experimental standard redox electrode potential $E^\circ(\text{expt})$ is also listed for comparison. The ΔG°_1 value of $-36.06 \text{ kcal mol}^{-1}$ is in good agreement with experimental value of $-36.94 \text{ kcal mol}^{-1}$. The theoretical values 0.782 and 0.815 V of $E^\circ_1(\text{calcd})$ and $E^\circ_2(\text{calcd})$ at the B3LYP/6-311++G(d,p) level show very small deviations (0.019 and 0.014 V) compared with the experimental value 0.801 V of $E^\circ(\text{expt})$ and the discrepancies are less than the values reported for other quinone derivatives [24, 26]. The calculated results are in reasonable agreement with the experimental value. $E^\circ_1(\text{calcd})$, $E^\circ_2(\text{calcd})$ and $E^\circ(\text{expt})$ are in accordance with the previous data obtained by Song Yuan-zhi etc [27]. This consistency certifies that the theoretical level is adequate and the CPCM solvation model is valid for calculating the solvation energies of the studied molecule.

4.4. Experimental and theoretical studies of DA-Gly/DAquinone-Gly couple

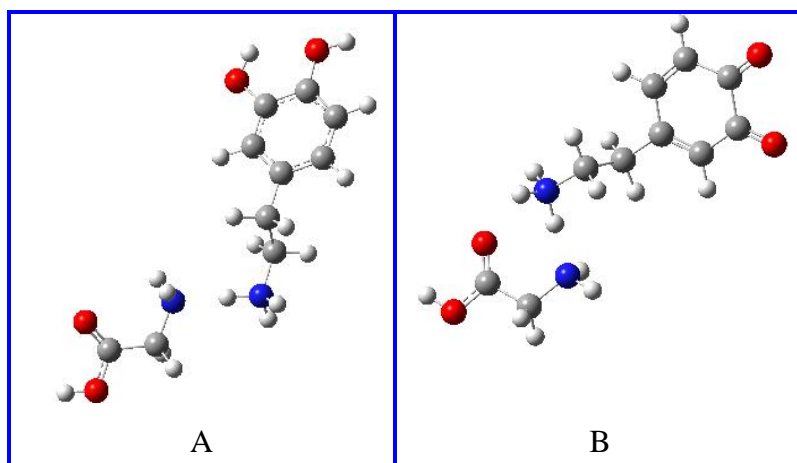


Figure 6. The most stable H-bonded complexes DA-Gly (A) and DAquinone-Gly (B) optimized in aqueous solution at the B3LYP/6-311++G(d,p) level.

Tugsuz has theoretically calculated the standard electrode potentials of imidazole dimer, tetrathiafulvalene dimer and tetrathiafulvalene-imidazole supramolecules, and his work shows that the redox potentials of supramolecules can be predicted accurately with theoretical methods [28]. In the present work, Gly is chosen as the model molecule to study the electron transfer properties of DA in physiological environment. We only consider the supramolecular complex with the 1:1 ratio of DA and Gly, which is accurate enough to predicate potentials. To rationalize theoretical calculations, as done in Tugsuz's work [28], all initial geometries of DA-Gly and DAquinone-Gly obtained by attaching Gly to the phenolic hydroxyl group, amino group, and alcoholic hydroxyl group of DA and DAquinone are optimized fully in gas phase and aqueous solution at B3LYP level.

The most stable hydrogen bond complexes DA-Gly and DAquinone-Gly optimized in aqueous solution are shown in Fig. 6. The nitrogen atom in Gly is hydrogen bond acceptor for the carboxyl is an electron-withdrawing group, while amino groups are hydrogen bond donors in both of the most

stable structures. The Gibbs energies $G^\circ(\text{g})$ of each component in gas phase, solvation energies $\Delta G(\text{solv})$ calculated using CPCM model of solvation, the total changes of Gibbs free energy for reductive reaction I and II from Ox DAquinone-Gly to Red DA-Gly, ΔG°_3 and ΔG°_4 , are listed in Table 2. The calculated standard redox electrode potentials $E^\circ(\text{calcd})$ (vs SHE) for DA/DAquinone redox couple using methods I and II, $E^\circ_3(\text{calcd})$ and $E^\circ_4(\text{calcd})$, are 0.836 V and 0.869 V, respectively, which are much larger than $E^\circ_1(\text{calcd})$ and $E^\circ_2(\text{calcd})$, indicating that the hydrogen bond between DA and Gly can protect DA from being oxidated to DAquinone through dispersing the electron density of DA molecule.

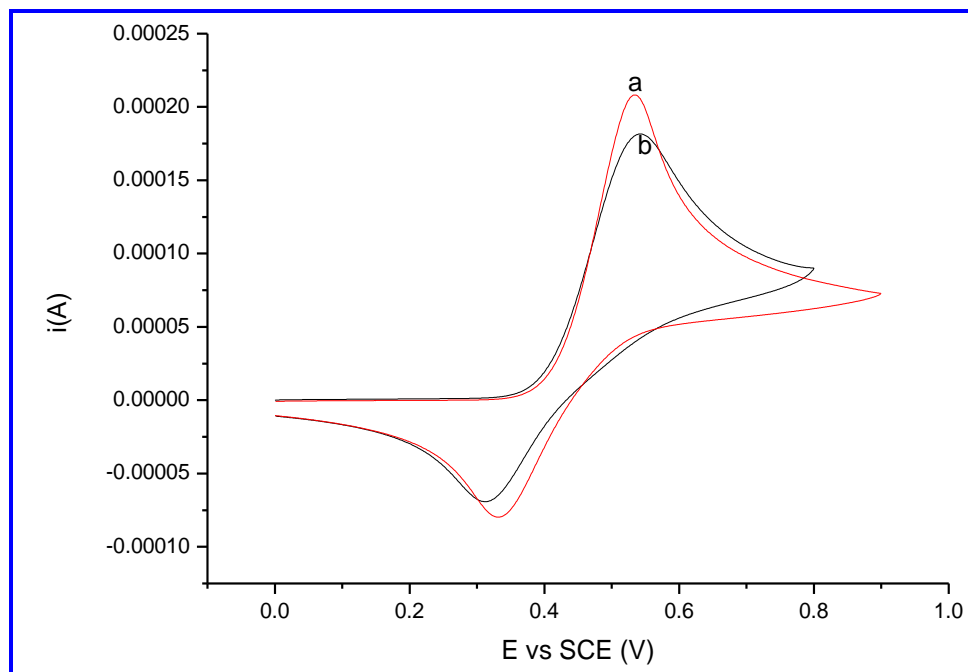


Figure 7. The CV behaviors of $5.2 \times 10^{-3} \text{ mol L}^{-1}$ DA in aqueous solution at GCE with a scan rate 100 mV/s. a: $C_{\text{DA}} = 5.2 \times 10^{-3} \text{ mol L}^{-1}$. b: $C_{\text{DA}} = 5.2 \times 10^{-3} \text{ mol L}^{-1}$ and $C_{\text{DA-Gly}} = 5.2 \times 10^{-3} \text{ mol L}^{-1}$.

To confirm the interaction between Gly and DA, the CV experiment is performed with different electrolytes of the same pH value at room temperature, simultaneously. In Fig. 10, curve a denotes the cyclic voltammogram of $5.2 \times 10^{-3} \text{ mol L}^{-1}$ DA in buffer solutions (pH=2.2) and b denotes the cyclic voltammograms of the mixture solution (pH=2.2) with $5.2 \times 10^{-3} \text{ mol L}^{-1}$ DA and $5.2 \times 10^{-3} \text{ mol L}^{-1}$ Gly at GCE. It is not hard to find that the anodic peak potential of a is smaller than that of b, and the anodic peak current of a is larger than that of b. We have performed lots of experiments to determine the accurate $E^\circ(\text{expt})$ (vs SHE) value of DA-Gly/DAquinone-Gly. The average value 0.819 V of $E^\circ(\text{expt})$ is larger than $E^\circ(\text{expt})$ (vs SHE) 0.801 V of DA/DAquinone. The phenomenon suggests that Gly in solution weakens the electron-donating ability of DA through the hydrogen bond interaction, which is in reasonable agreement with the theoretical results. Thus, theoretical methods are proved to be valid to predict the ease or complexity of certain materials' redox reaction. The method I gives results closer to the experimental values here, and our result agrees with Tugsuz's [28] at this point.

5. CONCLUSION

In the present article, two redox couples, DA/DAquinone and DA-Gly/DAquinone/Gly, have been studied by CV experiments and B3LYP calculations. Experimentally, the standard potentials E° (vs SHE) of DA/DAquinone couple is 0.801 V derived from the linear relationship between E° and pH. Theoretically, the standard potentials E° of DA/DAquinone is 0.784 V calculated with method I, and 0.815 V calculated with method II. Theoretical calculations are in good agreement with the experiments.

At the same time, the microenvironment effect on the oxidation of DA has been studied by choosing Gly as the model molecule. The theoretical redox potentials of DA-Gly/DAquinone-Gly system are higher than that of DA/DAquinone calculated via two methods at B3LYP/6-311++G(d,p) level. The experimental results verify the theoretical conclusion that the hydrogen bond interaction weakens the electron-donation ability of DA, which can be obtained from the phenomena that Gly decreases the oxidation currents of DA, and increases its redox potentials.

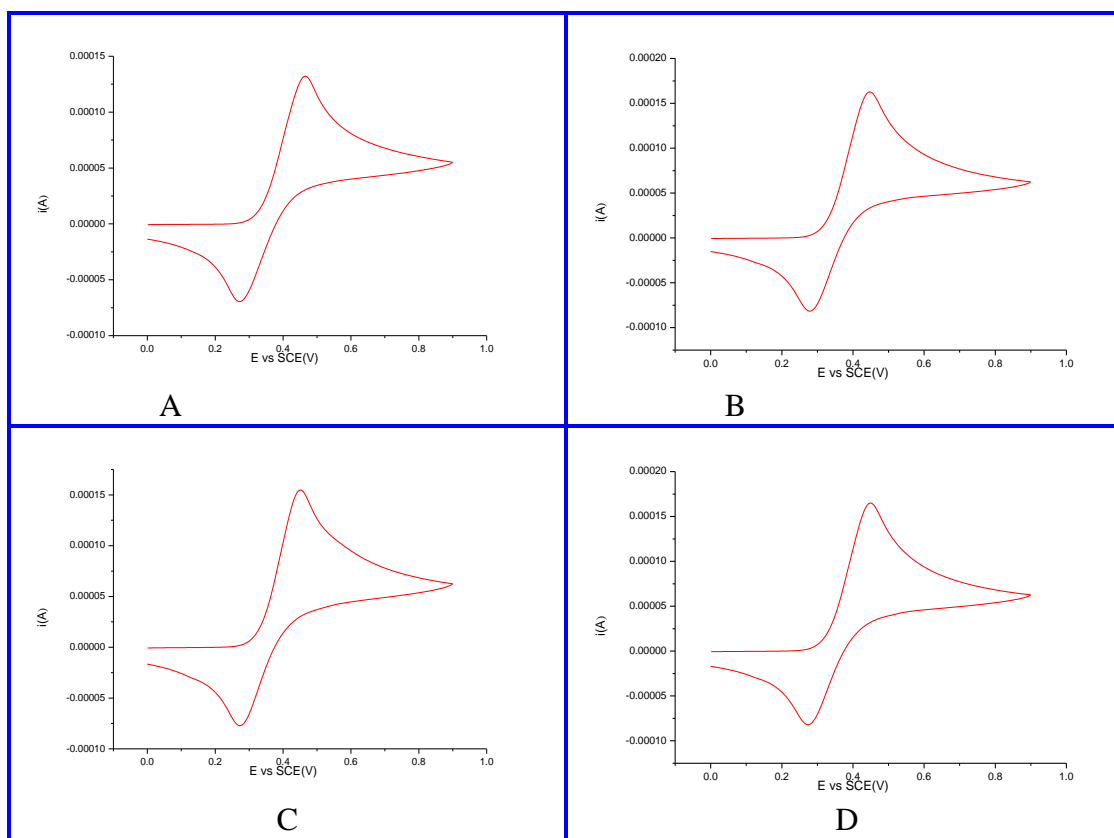
ACKNOWLEDGEMENTS

This work was jointly supported by National Natural Science Foundation of China (No. 21303073) and the Natural Science Foundation of Shandong Province (No. ZR2013BL005).

References

1. A. Carlsson, *Pharmacol. Rev.*, 11 (1959) 490.
2. C.A. Barraclough, P.M. Wise, *Endocr. Rev.*, 3 (1982) 91.
3. H. Bernheimer, W. Birkmayer, O. Hornykiewicz, K. Jellinger, F. Seitelberger, *J. Neurol. Sci.*, 20 (1973) 415.
4. N.E. Andén, S.G. Butcher, H. Corrodi, K. Fuxe, U. Ungerstedt, *Eur. J. Pharmacol.*, 11 (1970) 303.
5. C. A. Reynolds, W. G. Richards, P. J. Goodford, *Anticancer Drug Des.*, 1 (1987) 291.
6. P. Gurusamy, K. Muthukumar, S. Rajesh, G. Muneeswaran, S. Perumal, C. Karunakaran, *J. Struct. Biol.*, 180 (2012) 125.
7. R. Djemil, D. Khatmi, *J. Comput. Theor. Nanos.*, 9 (2012) 1571.
8. Z.G. Huang, Y.M. Dai, L. Yu, H.K. Wang, *J. Mol. Model.*, 7 (2011) 2609.
9. Z.Y. Yu, X.C. Li, X.L. Wang, J.J. Li, K.W. Cao, *Int. J. Electrochem. Sci.*, 6 (2011) 3890.
10. Z.Y. Yu, X.C. Li, X.L. Wang, X.Y. Ma, X. Li, K.W. Cao, *J. Chem. Sci.*, 124 (2012) 537.
11. M.A. Mohammad, B. Hadi, K.A. Mohammad, M. Fakhradin, B.F. Mirjalili, *Biosens. Bioelectron.*, 26 (2011) 2102.
12. Y. Li, Y. Umasankar, S. M. Chen, *Anal. Biochem.*, 388 (2009) 288.
13. C. Wang, R. Yuan, Y.Q. Chai, S.H. Chen, F.X. Hu, M.H. Zhang, *Anal. Chim. Acta.*, 741 (2012) 15.
14. F. Cui, X.L. Zhang, *J. Electroanal. Chem.*, 669 (2012) 35.
15. A.J. Bard, L.R. Faulkner, *Electrochemical Methods: Fundamentals and Applications*, Wiley: New York (2001).
16. M.J. Frisch, G.W. Trucks, H.B. Schlegel, G.E. Scuseria, M.A. Robb, J.R. Cheeseman, G. Scalmani, V. Barone, B. Mennucci, G.A. Petersson, H. Nakatsuji, M. Caricato, X. Li, H.P. Hratchian, A.F. Izmaylov, J. Bloino, G. Zheng, J.L. Sonnenberg, M. Hada, M. Ehara, K. Toyota, R. Fukuda, J. Hasegawa, M. Ishida, T. Nakajima, Y. Honda, O. Kitao, H. Nakai, T. Vreven, J. Montgomery, J.E. Peralta, F. Ogliaro, M. Bearpark, J.J. Heyd, E. Brothers, K. N. Kudin, V.N. Staroverov, R. Kobayashi, J. Normand, K. Raghavachari, A. Rendell, J.C. Burant, S. S. Iyengar, J.

- Tomasi, M. Cossi, N. Rega, N. J. Millam, M. Klene, J. E. Knox, J. B. Cross, V. Bakken, C. Adamo, J. Jaramillo, R. Gomperts, R.E. Stratmann, O. Yazyev, A.J. Austin, R. Cammi, C. Pomelli, J.W. Ochterski, R.L. Martin, K. Morokuma, V.G. Zakrzewski, G.A. Voth, P. Salvador, J. J. Dannenberg, S. Dapprich, A.D. Daniels, € O. Farkas, J. B. Foresman, J.V. Ortiz, J. Cioslowski, D.J. Fox, Gaussian 09, Revision A.1, Gaussian, Inc., Wallingford, CT, 2009.
17. V. Barone, M. Cossi, *J. Phys. Chem. A*, 102 (1998) 1995.
 18. M. Cossi, N. Rega, G. Scalmani, V. Barone, *J. Comput. Chem.*, 24 (2003) 669.
 19. Y. Takano and K. N. Houk, *J. Chem. Theor. Comput.*, 1 (2005) 70.
 20. M.D. Liptak, K.C. Gross, P.G. Seybold, S. Feldgus and G.C. Shields, *J. Am. Chem. Soc.*, 124 (2002) 6421.
 21. M. Eslami, H.R. Zare and M. Namazian, *J. Phys. Chem. B*, 116 (2012) 12552.
 22. J. Wang, *Analytical Electrochemistry*, John Wiley & Sons, New York (2006).
 23. G. W. Gokel, *Dean's Handbook of Organic Chemistry*, McGrawHill, New York (2004).
 24. M. Eslami, M. Namazian, H. R. Zare, *J. Phys. Chem. B*, 117 (2013) 2757.
 25. A. Albert, E.P. Serjeant, *The determination of ionization constants*, London, Chapman and Hall, (1971).
 26. M. Namazian, H. R. Zare, M. L. Coote, *Biophys. Chem.*, 132 (2008) 64.
 27. Y.Z. Song, Y. Song, *Can. J. Chem.*, 84 (2006) 1084.
 28. T. Tugsuz, *J. Phys. Chem. B*, 114 (2010) 17092.



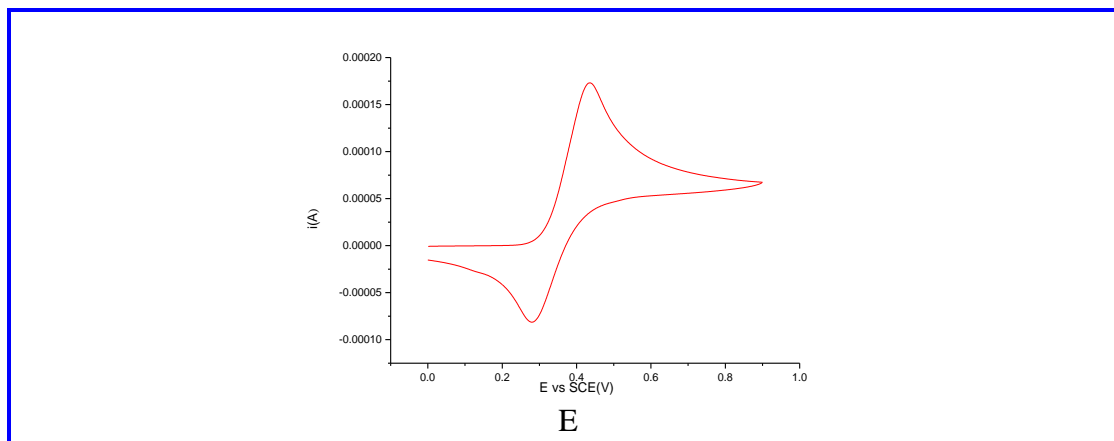


Figure S1. The CV behaviors of $5.2 \times 10^{-3} \text{ mol L}^{-1}$ DA at GCE in phosphate buffer solution of fixed pH 3.2 with various temperature values at a scan rate of 100 mV/s (A to E: temperature (T)=293.15, 298.15, 303.15, 308.15, 311.15 K)

© 2015 The Authors. Published by ESG (www.electrochemsci.org). This article is an open access article distributed under the terms and conditions of the Creative Commons Attribution license (<http://creativecommons.org/licenses/by/4.0/>).